

## Ion Pair First and Second Acidities of Some $\beta$ -Diketones and Aggregation of Their Lithium and Cesium Enediolates in THF

Antonio Facchetti<sup>†</sup> and Andrew Streitwieser<sup>\*,‡</sup>

Department of Chemistry, University of California, Berkeley, California 94720-1460, and Department of Chemistry and the Materials Research Center, Northwestern University, Evanston, Illinois 60208-3113

astreit@socrates.berkeley.edu

Received May 13, 2004

Ion pair  $pK$  values were measured for three  $\beta$ -diketones in THF, **1–3**, with lithium and cesium counterions. The results showed variations with concentration indicative of aggregation of the metal enolates to dimers. Similarly, ion pair  $pK$  values could be determined for some of these metal enolates going to the corresponding dimetal dienediolates which were also found to form dimers. These equilibria are more complicated to analyze because aggregation affects both sides of the proton transfer equilibria. The results show that all of the species measured exist mostly as dimers at concentrations  $>0.01$  M typical of most organic synthesis reactions and physical measurements. NMR measurements show that the enols of **1** and **2**, which can undergo intramolecular hydrogen bonding, predominate in both THF and DMSO solutions, whereas **3**, whose enols cannot be so stabilized, is mostly keto in THF but approximately equimolar enol and keto in DMSO. Dimerization of the monolithium salts is rapid on the NMR time scale but that of the dilithium salts is slow.

### Introduction

$\beta$ -Dicarbonyl functions in aldehydes, esters, or ketones can generally be deprotonated stepwise between the carbonyl groups to give monoanions and then at the external ketone enolate site to give 1,3-dienediolate dianions. Mono-<sup>1</sup> and dianions<sup>2,3</sup> arising from the mono- or bis-deprotonation of  $\beta$ -dicarbonyl compounds have been widely used in organic synthesis because of their ready access, predictable reactivity, and expanded reaction repertoire. Several reviews have covered the preparation and reactivity of these systems; their use is commonplace in total synthesis and methodology as a reliable tool when three-, four-, or five-carbon-chain extension is required. Alkylation reactions of mono-<sup>4–8</sup> and dienediolates<sup>2,9,10</sup> of  $\beta$ -dicarbonyl compounds with alkyl halides continue to be attractive pathways to substituted ketoesters and diketones as well as novel oxygen-<sup>11,12</sup> and nitrogen-containing<sup>12,13</sup> heterocycles. Epoxides have also been used extensively as alkylating

reagents for  $\beta$ -dicarbonyl dianions.<sup>14–17</sup> Aldol addition reactions<sup>2,4,18</sup> of these dianions have been explored to a lesser degree than alkylation. However, the aldol products can spontaneously cyclize to hemiketals or lactones depending on the nature of the dianion and this property has been exploited in the preparation of novel oxygen-based heterocycles. Yumaguchi and co-workers have made extensive use of the acylation of  $\beta$ -dicarbonyl dianions in the synthesis of polyketides, phenols, and aryl C-glucosides.<sup>16</sup> The dianions of simple  $\beta$ -diketones have been acylated and used in the synthesis of stegobinone<sup>19</sup> and xanthenes.<sup>20</sup>

Metal enolates of ketones, amides, esters, and other carbon derivatives are known to be frequently aggregated in ethereal solvents and in recent years this group has determined a number of such aggregation equilibrium constants and the relative ion pair acidities of the monomers.<sup>21–32</sup> Recently, the general approach was ap-

\* Address correspondence to this author.

<sup>†</sup> Northwestern University.

<sup>‡</sup> UC Berkeley.

(1) House, H. O. *Modern Synthetic Reactions*; W. A. Benjamin, Inc.: Menlo Park, CA, 1972.

(2) Thompson, C. M.; Green, D. L. C. *Tetrahedron* **1991**, *47*, 4223–4285.

(3) Thompson, C. M. *Dianion Chemistry in Organic Synthesis*; CRC Press: Boca Raton, FL, 1994.

(4) Caine, D. In *Carbon–Carbon Bond Formation*; Marcel Dekker: New York, 1979; Vol. 1, pp 90–341.

(5) Li, C.-J.; Lu, Y.-Q. *Tetrahedron Lett.* **1995**, *36*, 2721.

(6) Ranu, B. C.; Bhar, S. J. *Chem. Soc., Perkin Trans. 1* **1992**, 385.

(7) Antonioletti, R.; Bonadies, F.; Orelli, L. R.; Scettri, A. *Gazz. Chim. Ital.* **1992**, 237.

(8) Shone, T.; Kashimura, S.; Sawamura, M.; Soejima, T. *J. Org. Chem.* **1988**, *53*, 907.

(9) Harris, T. M.; Harris, C. M. *Org. React.* **1969**, *17*, 1.

(10) Kaiser, E. M.; Petty, J. D.; Knutson, P. L. A. *Synthesis* **1979**, 509.

(11) Marzinzik, A. L.; Felder, E. R. *Molecules* **1997**, *2*, 17.

(12) Nasibov, S. S.; Sadykhov, N. S.; Muradava, F. M. *Russ. Chem. Bull.* **1997**, *46*, 1618.

(13) Osowska-Pacewicka, K.; Zwierzak, A. *Synth. Commun.* **1988**, *28*, 1127–1137.

(14) Kowalski, C.; Haque, M. S.; Fields, K. W. *J. Am. Chem. Soc.* **1985**, *107*, 1429.

(15) Mori, K.; Sasaki, M.; Tamada, T.; Suguro, T.; Masuda, S. *Heterocycles* **1978**, *10*, 111.

(16) Yamaguchi, M.; Hirao, I. *Chem. Lett.* **1985**, 337.

(17) Lygo, B. *Tetrahedron* **1988**, *44*, 6889.

(18) Peterson, J. R.; Winter, T. J.; Miller, C. P. *Synth. Commun.* **1988**, *28*, 949.

(19) Gil, P.; Razkin, J.; Gonzalez, A. *Synthesis* **1998**, *4*, 386.

(20) Chandrasekhar, B.; Ramadas, S. R.; Ramana, D. V. *Tetrahedron* **2000**, *56*, 5947.

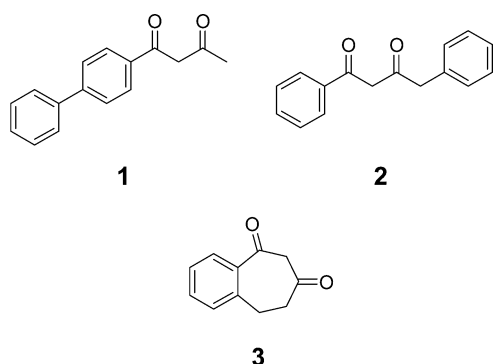
(21) Abbotto, A.; Streitwieser, A. *J. Am. Chem. Soc.* **1995**, *117*, 6358–6359.

(22) Abu-Hasanayn, F.; Stratakis, M.; Streitwieser, A. *J. Org. Chem.* **1995**, *60*, 4688–4689.

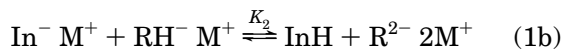
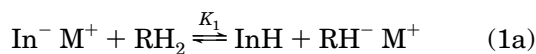
(23) Gareyev, R.; Ciula, J. C.; Streitwieser, A. *J. Org. Chem.* **1996**, *61*, 4589–4593.

plied to the lithium and cesium enediolates of an aryl-acetic acid,<sup>33</sup> which were found to form tight dimers.

The knowledge of the actual reactive species involved in reactions of such systems is fundamental for mechanism hypotheses and particularly to understand reaction stereochemistry. Accordingly, in this paper we applied these approaches to the lithium and cesium enolates of the dicarbonyl systems **1–3**. Since UV–vis spectroscopy was a principal tool in this study, the aryl groups were required as chromophores. Moreover, at the low concentrations inherent in UV–vis measurements, addition of the anions to carbonyl groups was slow and did not affect our study. Compound **1** has a terminal methyl group for forming the dianion whereas in **2** the dianion has further conjugation. Both of these compounds form monoanion ion pairs expected to be of U-shape.<sup>34</sup> To compare with a system constrained to a W-shape we included compound **3**.



As described previously, the ion pair acidity difference between a given system and a reference indicator is defined by the equilibrium in eq 1 with the corresponding  $pK$  difference given by eq 2.<sup>35</sup>



$$\Delta pK = -\log K_1 = pK[\text{RH}_2] - pK[\text{InH}] \quad (2)$$

In the present case, two protons can be removed to give first and second equilibrium constants and  $\Delta pK$  values.

(24) Krom, J. A.; Streitwieser, A. *J. Org. Chem.* **1996**, *61*, 6354–6359.

(25) Streitwieser, A.; Krom, J. A.; Kilway, K. A.; Abbotto, A. *J. Am. Chem. Soc.* **1998**, *120*, 10801–10806.

(26) Streitwieser, A.; Wang, D. Z.; Stratakis, M. *J. Org. Chem.* **1999**, *64*, 4860–4864.

(27) Streitwieser, A.; Wang, D. Z.-R. *J. Am. Chem. Soc.* **1999**, *121*, 6213–6219.

(28) Wang, D. Z.-R.; Streitwieser, A. *Can. J. Chem.* **1999**, *77*, 654–658.

(29) Wang, D. Z.; Kim, Y.-J.; Streitwieser, A. *J. Am. Chem. Soc.* **2000**, *122*, 10754–10760.

(30) Streitwieser, A.; Kim, Y.-J.; Wang, D. Z.-R. *Org. Lett.* **2001**, *3*, 2599–2601.

(31) Abbotto, A.; Leung, S. S.-W.; Streitwieser, A.; Kilway, K. V. *J. Am. Chem. Soc.* **1998**, *120*, 10807–10813.

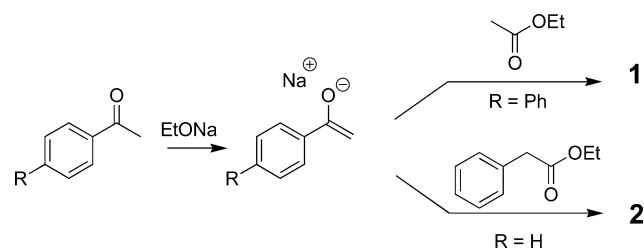
(32) Facchetti, A.; Streitwieser, A. *J. Org. Chem.* **1999**, *64*, 2281–2286.

(33) Streitwieser, A.; Husemann, M.; Kim, Y.-J. *J. Org. Chem.* **2003**, *68*, 7937–7942.

(34) Zaugg, H. E.; Schaefer, A. D. *J. Am. Chem. Soc.* **1965**, *87*, 1857–1866.

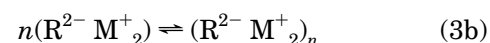
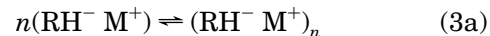
(35) Bors, D. A.; Kaufman, M. J.; Streitwieser, A., Jr. *J. Am. Chem. Soc.* **1985**, *107*, 6975–6982.

## SCHEME 1



The resulting  $\Delta pK$  values are converted for convenience to absolute numbers<sup>36</sup> by setting the  $pK$  of fluorene equal to its ionic  $pK_a$  of 22.9 (per hydrogen) in DMSO.<sup>37</sup> We have emphasized previously that such “ion pair  $pK$  values” are not  $pK_a$  values.<sup>38</sup>

Since all of the indicator anions are known to exist exclusively as monomeric ion pairs in THF, the indicator technique can be used to determine the presence of substrate anion ion pair aggregates. Aggregation of the enolate ion pairs, eq 3, pulls equilibrium 1 to the right resulting in an observed  $pK$  value lower than that in the absence of aggregation. In addition, due to the stoichiometry of eq 3, the effect of enolate aggregation is to increase the observed acidity of the corresponding acidic partner as the total enolate concentration is increased. In this paper we employ this principle to determine the ion pair acidities of lithium and cesium mono- and dienolates of compounds **1–3** and to study their degrees of aggregation in THF solution. We compare these results with other classes of organic compounds previously studied in this laboratory.



Finally, <sup>1</sup>H and <sup>13</sup>C NMR studies in THF-*d*<sub>8</sub> and DMSO-*d*<sub>6</sub> provide structural details of the neutral and anionic species derived from **1–3**.

## Results

**Synthesis.** 1-(4-Biphenyl)butane-1,3-dione (**1**)<sup>39</sup> and 1,4-diphenylbutane-1,3-dione (**2**)<sup>40</sup> were prepared with slight modifications of known procedures according to Scheme 1. Phenyl- and 4-biphenyl methyl ketone were deprotonated with EtONa in ethanol and reacted with ethyl acetate or ethyl phenylacetate, respectively, to afford the corresponding diketones **1** or **2** in high yields.

To the best of our knowledge, cyclic diketone **3** is unknown in the literature. It was prepared starting from 3-(2-acetylphenyl)propionic acid, which was converted into the corresponding ethyl ester by reaction with SOCl<sub>2</sub> and quenching with ethanol. Cyclization of the ketoester (Scheme 2) was performed in refluxing *t*-BuOH with *t*-BuOK as base.

(36) Kaufman, M. J.; Gronert, S.; Streitwieser, A., Jr. *J. Am. Chem. Soc.* **1988**, *110*, 2829–2835.

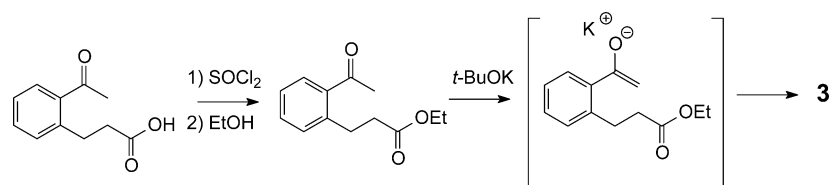
(37) Bordwell, F. G. *Acc. Chem. Res.* **1988**, *21*, 456–463.

(38) Streitwieser, A.; Kim, Y.-J. *J. Am. Chem. Soc.* **2000**, *122*, 11783–11786.

(39) Sprague, J. M.; Beckham, L. J.; Adkins, H. *J. Am. Chem. Soc.* **1934**, *56*, 2665–2668.

(40) Padwa, A.; Hornbuckle, S. F.; Zhang, Z.; Zhi, L. *J. Org. Chem.* **1990**, *55*, 5297.

## SCHEME 2

**TABLE 1. Spectroscopic Data for Lithium and Cesium Enolates of 1–3 in THF at 25 °C**

compd	enolates	$\lambda_{\max}$ (nm)	$\epsilon$ (cm <sup>-1</sup> M <sup>-1</sup> )
<b>1</b>	-H	324	29 600
	-Li	340–342 <sup>a</sup>	21 500
	-Li <sub>2</sub>	379–381 <sup>a</sup>	12 950
	-Cs	350–355 <sup>a</sup>	17 500
	-Cs <sub>2</sub>	418–421 <sup>a</sup>	8 800
<b>2</b>	-H	312	18 300
	-Li	333	19 500
	-Li <sub>2</sub>	400–402 <sup>a</sup>	19 400
	-Cs	338–340 <sup>a</sup>	15 900
	-Cs <sub>2</sub>	430–438 <sup>a</sup>	24 700
<b>3<sup>c</sup></b>	-H	444 <sup>b</sup>	23 600
	-Li	<290	
	-Li	329	13 300
	-Li <sub>2</sub>	337	3 430
	-Cs	336	11 000 <sup>d</sup>

<sup>a</sup> Depending on concentration. <sup>b</sup> Data are for the isosbestic point. <sup>c</sup> Dicesium enolate is not soluble. <sup>d</sup> Monocesium enolate is poorly soluble.  $\epsilon$  is  $\pm 20\%$ .

**UV–vis Measurements: Ion Pair Absorption Spectra.** With the exception of **3** and its completely insoluble dicesium enolate **3**-Cs<sub>2</sub>, all of the neutral, monometal, and dimetal enolates (metal = Li, Cs) of  $\beta$ -dicarbonyl compounds **1–3** were found to absorb in the visible or near-UV region in THF (Figures S1–S3, Supporting Information). The extinction coefficient ( $\epsilon$ ) of each ion pair was determined by recording a series of 22–35 absorption spectra at different metal enolate concentrations (Figures S4–S14, Supporting Information). A detailed description is reported in the Experimental Section. Due to its poor solubility, the extinction coefficient of the cesium enolate **3**-Cs was obtained at very low anion concentrations, which prevented further dilution for each experiment. For this reason, this value has lower accuracy because only five absorption spectra were obtained (Figure S15, Supporting Information). The absorption spectra of mono-enolates **1**-Li, **1**-Cs, and **2**-Cs were found to be slightly concentration dependent, with a shift of the maximum absorption ( $\lambda_{\max}$ ) ranging from 2 to 5 nm. For the dienediolates of **1** and **2** the shift of  $\lambda_{\max}$  ranges from 2 to 8 nm. No appreciable shift was observed for the other enolate systems. Extinction coefficient measurements of **2**-Cs<sub>2</sub> at varying concentrations reveal an isosbestic point at 444 nm (vide infra). No clear isosbestic point could be detected for the other enolates, probably because the concentration dependencies of their spectra are smaller than the experimental error in the measurements. In Table 1 are collected the spectroscopic data,  $\lambda_{\max}$ , and extinction coefficient at  $\lambda_{\max}$  and/or at the isosbestic point of neutral systems **1** and **2**, and of the soluble lithium and cesium enolates of **1–3**.

**Ion Pair Acidity.** The lithium and cesium ion pair acidities of the dicarbonyl systems **1–3** were measured against hydrocarbon indicators (Table 2) with known  $pK$ . The cesium scale<sup>41,42</sup> involves contact ion pairs (CIP),<sup>36</sup>

whereas the lithium scale<sup>42,43</sup> involves solvent-separated ion pairs (SSIP). In the case of dienediolates (**1**, **2**)-Li<sub>2</sub> and (**1**, **2**)-Cs<sub>2</sub>, both ion pairs involved in eq 1 exhibit sufficiently distinct visible absorption spectra so that the concentrations of the species at equilibrium could be determined by the use of the double-indicator method. In this technique the concentrations of the ion pairs are determined by linear least-squares fitting of the spectra of the separate species (indicator and enolate) to the spectrum of the equilibrium mixture. In contrast, the mono-enolates (**1–3**)-Li and (**1–3**)-Cs and the dienediolate **3**-Li<sub>2</sub> do not have absorption maxima in the visible region. Although these enolate ion pairs exhibit distinct absorption in the near-UV, this region of the spectrum cannot be analyzed quantitatively due to the large number of overlapping peaks arising from both indicators and the neutral dicarbonyl substrates (see Figures S1–S3, Supporting Information). Consequently, we used the single indicator technique in which the spectrum of the indicator salt of known  $pK$  is recorded and the initial anion concentration is determined from the absorbance at the appropriate  $\lambda_{\max}$ . A measured amount of substrate RH<sub>2</sub> is then added and the equilibrium concentration of the indicator is determined directly from the new absorbance value. The equilibrium enolate concentration is then calculated with eq 4.

$$\{\text{RH}^- \text{M}^+\}_{\text{eq}} = [\text{In}^- \text{M}^+]_{\text{initial}} - [\text{In}^- \text{M}^+]_{\text{eq}} \quad (4)$$

Details on the single<sup>44</sup> and double<sup>36</sup> indicator methods were reported previously.

Initially we ensured that  $pK$  measurements would not be affected by the base employed to deprotonate the indicator or the mixture indicator–substrate. Reproducible  $pK$  results showed that a nitrogen-containing base such as diisopropylamine does not influence equilibrium **1** by forming aggregates with lithium enolates. Moreover, strong nucleophiles such as DPMCs or TMSLi do not react either with the dicarbonyl or with the mono-enolcarbonyl species. However, it is important in determining the acidity of dicarbonyl systems to simultaneously maintain an equilibrium concentration of either mono- or dimetalated enolate and the corresponding conjugate acid. This represents a potential problem since enolate ions can add to carbonyl groups. Furthermore, in principle, addition of the indicator anion to the C=O bond might also occur. This could be particularly true for those  $\beta$ -dicarbonyl

(41) Streitwieser, A.; Ciula, J. C.; Krom, J. A.; Thiele, G. *J. Org. Chem.* **1991**, *56*, 1074–1076.

(42) Facchetti, A.; Kim, Y.-J.; Streitwieser, A. *J. Org. Chem.* **2000**, *65*, 4195–4197.

(43) Streitwieser, A.; Wang, D. Z.; Stratakis, M.; Facchetti, A.; Gareyev, R.; Abbotto, A.; Krom, J. A.; Kilway, K. V. *Can. J. Chem.* **1998**, *76*, 765–769.

(44) Streitwieser, A., Jr.; Reuben, D. M. E. *J. Am. Chem. Soc.* **1971**, *93*, 1794–1795.

TABLE 2. Experimental Details To Measure Lithium and Cesium Ion Pair Acidities of Enolates 1–3

compd	enolates	base <sup>a</sup>	time (h) <sup>b</sup>	indicator <sup>c</sup> (pK, $\epsilon^d$ )	method <sup>e</sup>
1	-Li	TMSLi, LDA	4	DFB (5.61, 79 600)	S
	-Li <sub>2</sub>	LDA	48	BnFl (21.36, 15 400)	D
	-Cs	DPMCs, CuCs	5	BBP (12.29, 107 600)	S
	-Cs <sub>2</sub>	CumCs	<i>f</i>	TpTM (33.1, 30 200)	D
2	-Li	TMSLi	<i>f</i>	TPM (31.26, 29 900)	D
	-Li <sub>2</sub>	TMSLi	0.5	DFB	S
	-Li <sub>2</sub>	LDA	16	DMAPhFl (19.02, 27 800)	D
	-Cs	DPMCs	4	BBP	S
3	-Cs <sub>2</sub>	CumCs	0.5	DP5 (25.62, 117 000)	D
	-Li	TMSLi	0.25	DFB	S
	-Li <sub>2</sub>	LDA	60	2,3-BF (22.95, 25 500)	S
	-Cs	DPMCs	<i>f</i>	BBP	S

<sup>a</sup> Base for forming enolate: TMSLi, trimethylsilylmethylithium; LDA, lithium diisopropylamide; DPMCs, diphenylmethylcesium; CumCs, cumylcesium. <sup>b</sup> Approximate time to reach equilibrium. <sup>c</sup> Indicator for measurement: DFB, 3-(dibenzofulvenyl)-6-(9-fluorenyl)-1,2-benzofulvene; BnFl, 9-benzylfluorene; BBP, 1,3-bis(biphenylene)propene; TpTM, tri-*p*-tolylmethane; TPM, triphenylmethane; DMAPhFl, 9-dimethylaminophenylfluorene; DP5, 1,5-diphenyl-1,3-pentadiene; 2,3-BF, 2,3-benzofluorene. <sup>d</sup>  $\epsilon$  in  $\text{cm}^{-1} \text{M}^{-1}$ . <sup>e</sup> S, single indicator method. D, double indicator method. <sup>f</sup> These cesium enolates precipitate before an unchanging absorption spectrum of the equilibrating mixture was reached.

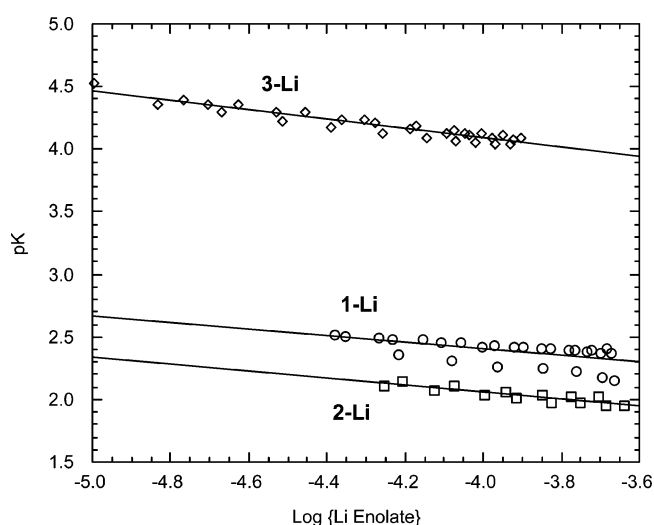


FIGURE 1. The pK values of the monolithium enolates vary with concentration. The regression lines are as follows: **1-Li**,  $1.34 \pm 0.27 - (0.265 \pm 0.068)x$ ; **2-Li**,  $0.952 \pm 0.142 - (0.277 \pm 0.036)x$ ; **3-Li**,  $2.58 \pm 0.095 - (0.376 \pm 0.022)x$ .

systems that are mainly present in THF solution as the keto tautomer. The tautomer equilibria will be discussed further in a later section. All of these secondary reactions would affect the position of the acid–base equilibrium and result in erroneous and irreproducible ion pair acidity values particularly in cases with long proton transfer equilibrium times. In practice, such secondary reactions were not an important problem, probably because of the high dilutions required for the UV–vis measurements. They might have contributed to the observed experimental uncertainties but these are relatively small, especially considering the difficulty of these measurements. Table 2 also shows the time needed to establish the proton-transfer equilibria. We assumed that the species present in eq 1 reached equilibrium when the UV–vis spectrum of the corresponding mixture did not change appreciably after 1 h. Previous work from this laboratory had shown<sup>23,45</sup> that proton transfer equilibria

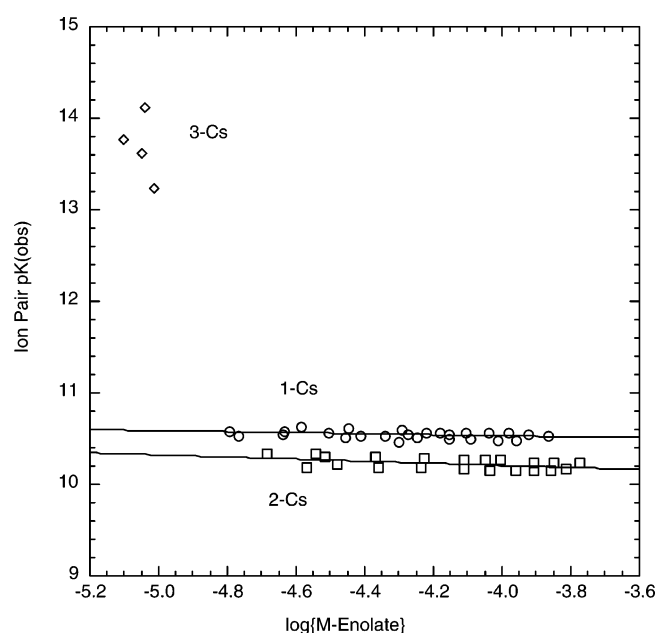


FIGURE 2. The pK values of the monocesium enolates vary with concentration. The regression lines are as follows: **1-Cs**,  $10.31 \pm 0.12 - (0.055 \pm 0.027)x$ ; **2-Cs**,  $9.75 \pm 0.18 - (0.115 \pm 0.044)x$ ; **3-Cs**, indeterminate because of solubility limitations.

between weak carbon acids are achieved much more rapidly with cesium compared to lithium counterions. The current study confirms this general trend. In fact, reactions involving the mono-/dilithium salts of **1–3** required long equilibration times probably because the Li–O bond is such a tight ion pair. On the other hand, the first deprotonations with lithium bases were found to be reasonably rapid.

**Monoenolates.** Plots of the observed ion pair acidities (pK values) vs the logarithm of the metal enolate concentration are presented in Figures 1 and 2. The pK values decrease with increasing concentration indicative of aggregation. The average aggregation numbers, *n*, given from the slopes (eq 5)<sup>35</sup> are summarized in

$$\text{pK}_{\text{obs}} = \frac{1-n}{n} \log\{\text{enolate}\} + b \quad (5)$$

(45) Xie, L.; Streitwieser, A. *J. Org. Chem.* **1995**, *60*, 1339–1346.

**TABLE 3.** Summary of Average Aggregation Numbers ( $n$ ), Dimerization Constants ( $K_{d,2}$ ), and Ion Pair  $pK$  Values of Lithium and Cesium Enolates of 1–3 in THF at 25 °C

compd	enolate	$n^a$	$K_d$ ( $M^{-1}$ )	$pK_o^b$
mono-enolates				
1	-Li	$1.23 \pm 0.02$	$2200 \pm 130$	2.58
	-Cs	$1.10 \pm 0.05$	$1000 \pm 200$	10.98
2	-Li	$1.36 \pm 0.05$	$5100 \pm 400$	2.27
	-Cs	$1.10 \pm 0.02$	$1050 \pm 100$	10.4
3	-Li	$1.61 \pm 0.05$	$26000 \pm 3000$	4.6
	-Cs	$-0.38 \pm 0.88$		$\sim 13$
dienolates				
1	-Li <sub>2</sub>	$1.43 \pm 0.03$	$6000 \pm 1000^d$	21.9
2	-Li <sub>2</sub>	$1.29 \pm 0.03$	$760 \pm 100^d$	17.7
	-Cs <sub>2</sub>	$1.06 \pm 0.02^c$	$140 \pm 20^d$	24.5

<sup>a</sup> Determined in the log concentration range of ca.  $-4.7$  to  $-3.3$ .

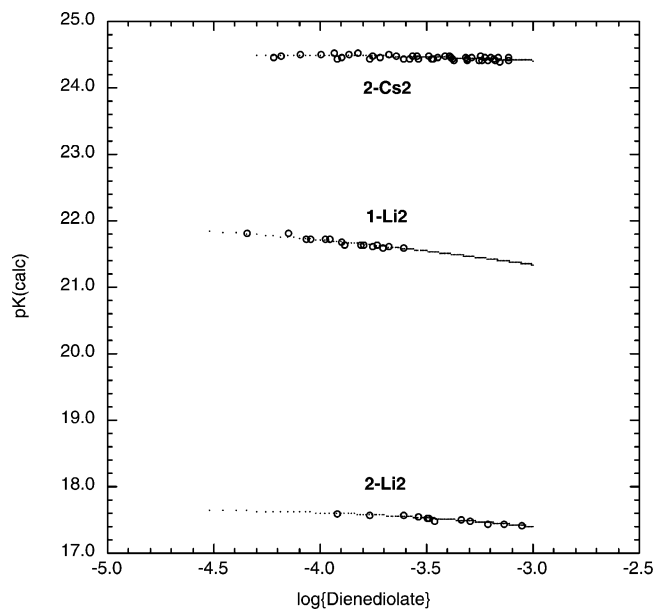
<sup>b</sup> For monomers; statistical effects in the carbonyl compounds are not considered. <sup>c</sup> Determined in the log concentration range of ca.  $-5.8$  to  $-4.2$  <sup>d</sup> Error bounds determined by statistics of the  $K_{obs}$  vs  $\{\text{dienediolate}\}/K_{obs}$  plots. Errors in  $K_{d,1}$  (for the mono-enolates) are not included.

Table 3. The modest values suggest that the aggregates are dimers. The scattering of points for **3**-Cs is a consequence of extreme dilution and no useful data could be extracted for this compound. Note also that throughout this paper concentrations expressed within curly brackets,  $\{\}$ , are formal concentrations as measured by spectroscopy.

For a monomer–dimer equilibrium an alternative expression of the data is by a plot of  $K_{obs}$  vs  $\{\text{enolate-M}\}/K_{obs}$ . The intercept gives  $K_o$  for the monomer and the slope is  $2K_dK_o^{2.24}$ . These plots are shown in Figures S17 and S18 (Supporting Information) and the calculated dimerization constants for the mono-enolate,  $K_{d,1}$ , are summarized in Table 3. The uncertainties are typically of the order of 10% but some uncertainties are substantially larger, probably because of the limitations of the single-indicator method.

Note that  $1/K_d$  is the concentration at which  $[\text{monomer}] = [\text{dimer}]$  and thus at concentrations  $>0.001$  M all of these mono-enolates are mostly dimer. These results suggest that most studies in the literature (e.g., NMR) of mono-enolates in THF actually pertain to the dimers. The dimerization constant for the W-enolate **3**-Li is much greater than that of the U-enolates **1**-Li and **2**-Li, undoubtedly because the latter monomers are stabilized by intramolecular coordination of lithium to both enolate oxygens. The comparable values for **1**-Cs and **2**-Cs suggest that the cesium enolate monomers are also importantly stabilized by such internal coordination.

**Dienediolates.** Application of these methods to the dialkali dienediolates by measuring the ion pair second acidity constants of the  $\beta$ -diketones is not so straightforward. The problem is that we must now consider aggregation in both the acid (the mono-enolate) and the base (the dienediolate). Aggregation of the acid increases the observed  $pK$  and aggregation of the base lowers it. In principle, one could calculate the amount of mono-enolate monomer from the now known  $K_{d,1}$  and formulate the acidity equilibria in terms of the monomer. In practice, this means having an indicator together with the diketone and enough strong base to convert part of the diketone to the dienediolate. The formal concentra-



**FIGURE 3.** The circles are experimental  $pK$  values for mono-enolate (as acid) and dienediolate (as base) monomers compared to points calculated from data in Tables 2 and 3 and from Figures S19–S21 (Supporting Information).

tion of dienediolate,  $\{\text{dienediolate}\}$ , together with the amount of indicator salt could generally be determined directly from the spectra. The formal mono-enolate concentration was then determined, in effect, by the single indicator technique. From  $K_{d,1}$  the mono-enolate concentration was deduced and used to determine the observed ion pair acidity equilibrium constant,  $K_{obs}$ , with the indicator of the second acidity constant of the ketone. A plot of  $K_{obs}/\{\text{RM}_2\}$  then gives  $K_o$  and the dimerization constant of the dimetalated ketone,  $K_{d,2}$ . This procedure could be applied to **1**-Li<sub>2</sub>, **2**-Li<sub>2</sub>, and **2**-Cs<sub>2</sub>, with the results summarized in Table 3. A few runs gave results inconsistent with the others and were discarded. The plots of  $K_{obs}$  vs  $K_{obs}/\{\text{dienediolate}\}$  used are shown in Figures S19–S21 (Supporting Information). The results were used to compute the calculated  $pK$  values for comparison with observed values as a function of  $\log\{\text{dienediolate}\}$  in Figure 3.

**<sup>1</sup>H NMR Data and Keto/Enol Tautomerism in Solution.** The  $pK$  measurements of the mono-enolates refer to the state of the diketone in solution, generally some equilibrating mixture of keto and enol tautomers.<sup>46,47</sup> To refer the acidities to the individual tautomers meant determining the keto–enol ratios. For example, aqueous solutions of acetylacetone have been extensively studied and were found at equilibrium to be approximately 20% enol at room temperature.<sup>48–50</sup> Base or solvent-promoted deprotonation of either keto or enol gives the same enolate anion. In our cases where the base is a metalated indicator, these equilibria are summarized in Scheme 3.

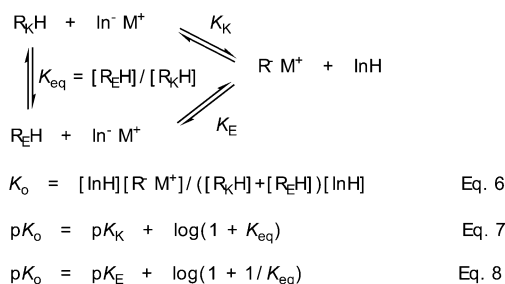
(46) Emsley, J.; Freeman, N. *J. Mol. Struct.* **1987**, *161*, 193.

(47) Bunting, J. W.; Kanter, J. P.; Nelander, R.; Wu, Z. *Can. J. Chem.* **1995**, *73*, 1305.

(48) Eidenhoff, M. L. *J. Am. Chem. Soc.* **1945**, *67*, 2073.

(49) Ahrenes, M. L.; Eigen, M.; Kruse, W. *Ber. Bunsen-Ges.* **1970**, *74*, 380.

(50) Moriyasu, M.; Kato, A.; Hashimoto, Y. *J. Chem. Soc., Perkin Trans. 2* **1986**, 515.

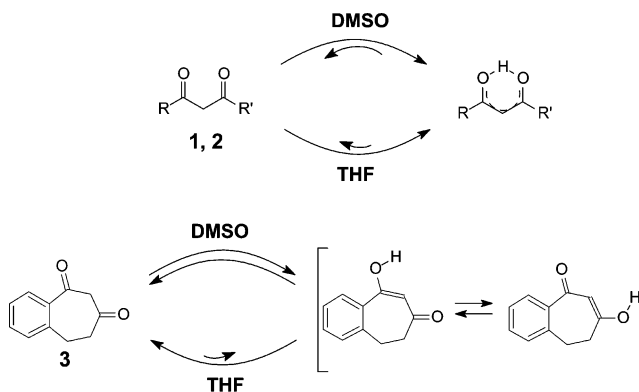
**SCHEME 3. Equilibria among Keto and Enol Forms and Conjugate Enolate Ion Pairs**

**TABLE 4.  $K_\text{eq}$  for the Keto–Enol Equilibria in THF and DMSO and Calculated  $\text{p}K_\text{K}$  and  $\text{p}K_\text{E}$  in THF at 25 °C**

compd	$K_\text{eq}^a$		$\text{p}K_\text{E}^{b,c}$		$\text{p}K_\text{K}^{b,c}$	
	THF	DMSO	-Li	-Cs	-Li	-Cs
1	11.74 ± 1.4	3.77 ± 0.4	2.54	10.94	1.48	9.88
2	113.47 ± 7.3	2.44 ± 0.1	2.27	10.4	0.21	8.3
3	0.082 ± 0.002	1.08 ± 0.1	3.42	~12	4.52	~13

<sup>a</sup> [enol]/[keto]. <sup>b</sup> Probable errors are about ±0.1 except for **3**-Cs, which are closer to ±1. <sup>c</sup> For monomeric enolates without consideration of statistical effects.

Important tools for measuring keto–enol equilibria have generally been <sup>1</sup>H NMR<sup>51,52</sup> and IR<sup>53</sup> spectroscopy. In most cases, the conversion rates between the two tautomers are sufficiently slow that the NMR spectra show separate and distinct proton signals of both the keto and enol tautomers. Hence, from the relative intensities of the signals the equilibrium concentrations of each of the two tautomers can be conveniently determined. <sup>1</sup>H NMR spectra of the neutral systems **1–3** (Figures S22–S24, Supporting Information) were recorded in dilute solution (0.01 M). THF and DMSO solutions were made up and allowed to reach tautomer equilibrium over a 1-day period. In both solvents the enol/keto composition could be determined by the integration of both keto and enol proton resonances. Integration of the signals with longer pulse delays (up to 10 s) gave similar results. The results of three experiments (Table S2, Supporting Information) were used to calculate  $K_\text{eq}$  and averaged in Table 4. From eqs 7 and 8,  $K_\text{K}$  and  $K_\text{E}$  were determined and combined with the  $\text{p}K_\text{O}$  results to give the ion pair acidity  $\text{p}K$  values for the keto and enol tautomers also summarized in Table 4.

The NMR investigation also points out the sensitivity of the keto/enol equilibrium to solvent polarity. It is widely recognized that this equilibrium has important kinetic implications in  $\beta$ -diketone reactivity.<sup>54</sup> For acyclic 1,3-diketones, polar solvents favor the more polar keto side of the equilibrium.<sup>55,56</sup> In agreement with these generalizations, we find that going from THF ( $\epsilon = 7.6$ ) to DMSO ( $\epsilon = 46.7$ ) the fractions of the enol form of **1** and **2** decrease from 92% and 99% to 79% and 71%,

**SCHEME 4. Keto–Enol Equilibria in DMSO and THF**


respectively. However, the enol form is largely the predominant species in both solvents. This result is not surprising considering that acyclic systems can form strong intramolecular hydrogen bonds (75 kJ mol<sup>-1</sup> for acetylacetone)<sup>57</sup> resulting in a stabilized cyclic enol structure (Scheme 4). The strength of this intramolecular bond would limit enol–solvent hydrogen bonding for most solvents. On the other hand, as discussed above, the W-shaped dicarbonyl moiety in **3** greatly affects the enol/keto equilibrium. In THF only 8% of the enol form of **3** is present, which increases to about 50% in DMSO. In this case, the more polar DMSO shifts the equilibrium to the enol side rather than to the ketone, probably because of intermolecular hydrogen bonding to the solvent of the open enol form(s); DMSO is a better hydrogen-bonding acceptor than THF.<sup>58</sup>

<sup>13</sup>C NMR Data and Geometric Isomerism in the Anions. Carbon NMR spectroscopy can provide further insights into the structures of **1–3** and of the corresponding enolate anions. Selected <sup>13</sup>C NMR resonances for all of the investigated systems in THF-*d*<sub>8</sub> and DMSO-*d*<sub>6</sub> are reported in Table 5. The spectra of the neutral and monolithium species were recorded in 0.1 M solutions whereas those of the dilithium dienediolates (**1**, **2**)-Li<sub>2</sub> were recorded as saturated solutions due to the poor solubility of these enolates. Unfortunately, **3**-Li<sub>2</sub> was too insoluble to be studied by NMR. Note that at 0.1 M concentration (**1–3**)-Li and (**1**, **2**)-Li<sub>2</sub> are all present almost wholly as dimers. Figures 4 and 5 (spectra A–C) show decoupled spectra of **1**, **2**, and the corresponding mono- and dilithium enolates in deuterated THF.

The NMR spectra of **1** and **2** exhibit one single set of resonances. The small amount of the keto form present was not detected (except for the C<sub>β</sub> of **1**). The internally hydrogen-bonded enols of  $\beta$ -diketones are known to be double-well systems<sup>59</sup> but the proton shift has a low barrier and is fast on the NMR time scale.<sup>60</sup> The decoupled (A) and coupled (B) <sup>13</sup>C NMR spectra of **3** in THF and DMSO are shown in Figures S25 (Supporting

(51) Reeves, L. W. *Can. J. Chem.* **1957**, *35*, 1351.

(52) Reeves, L. W.; Schneider, W. G. *Can. J. Chem.* **1958**, *36*, 793.

(53) Isaacs, N. S. *Experiments in Physical Organic Chemistry*; Macmillan: New York, 1969; p 132.

(54) Toullie, J., Ed. *Experiments in Physical Organic Chemistry*; Academic Press: London, UK, 1982.

(55) Emsley, J.; Freeman, N. J.; Parker, R. J.; Dawes, H. M.; Hursthouse, M. B. *J. Chem. Soc., Perkin Trans. 1* **1986**, 471.

(56) Emsley, J.; Freeman, N. J.; Bates, P.; Hursthouse, M. B. *J. Mol. Struct.* **1987**, *161*, 181.

(57) Emsley, J.; Freeman, N. J.; Parker, R. J.; Overill, R. E. *J. Chem. Soc., Perkin Trans. 1* **1986**, 1479.

(58) Matthews, W. S.; Bares, J. E.; Bartmess, J. E.; Bordwell, F. G.; Cornforth, F. J.; Drucker, G. E.; Margolin, Z.; McCallum, R. J.; McCollum, G. J.; Vanier, N. R. *J. Am. Chem. Soc.* **1975**, *97*, 7006.

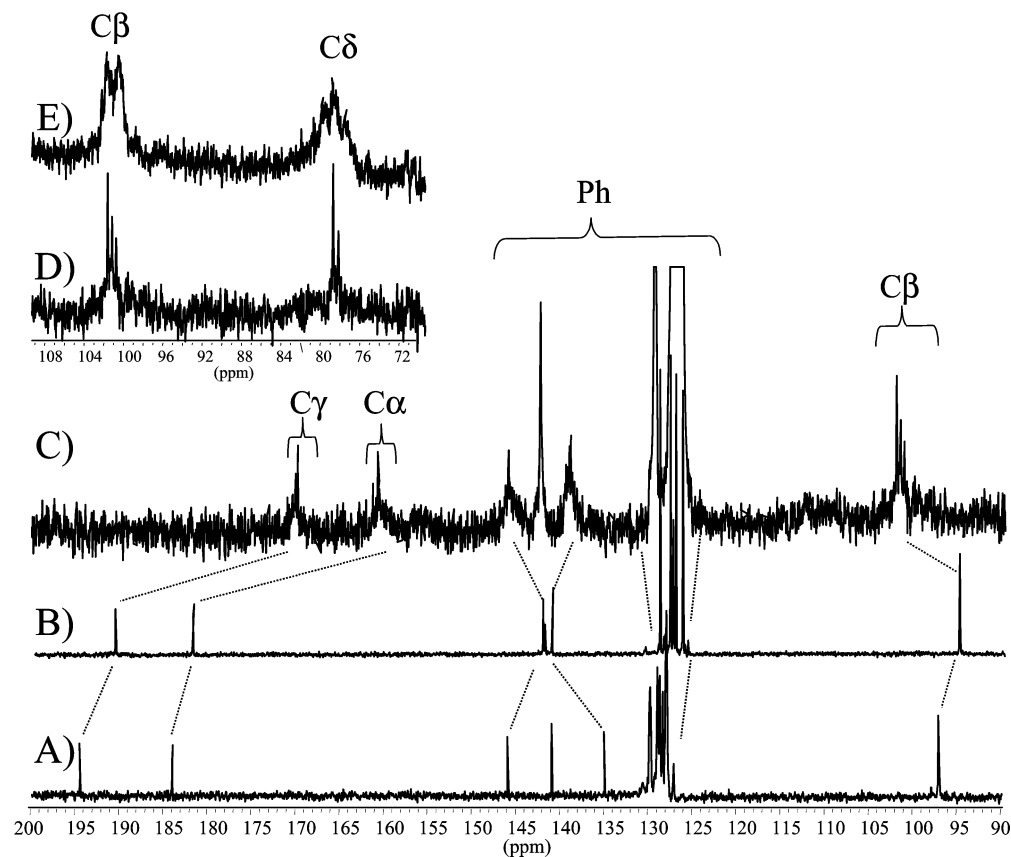
(59) Bauer, S. H.; Wilcox, C. F. *Chem. Phys. Lett.* **1997**, *279*, 122–128.

(60) Perrin, C. L.; Kim, Y.-J. *J. Am. Chem. Soc.* **1998**, *120*, 12641–12645.

**TABLE 5.**  $^{13}\text{C}$  and  $^1\text{H}$  NMR Chemical Shifts ( $\delta$ )<sup>a</sup> of 1–3 and of the Corresponding Mono-<sup>b</sup> and Dilithium<sup>c</sup> Enolates in THF-*d*<sub>8</sub> and DMSO-*d*<sub>6</sub> at 25 °C

compd	enolate	$^{13}\text{C}$ NMR								$^1\text{H}$ NMR					
		$\delta$ THF- <i>d</i> <sub>8</sub>				$\delta$ DMSO- <i>d</i> <sub>6</sub>				$\delta$ THF- <i>d</i> <sub>8</sub>			$\delta$ DMSO- <i>d</i> <sub>6</sub>		
		$\text{C}_\alpha$	$\text{C}_\beta$	$\text{C}_\gamma$	$\text{C}_\sigma$	$\text{C}_\alpha$	$\text{C}_\beta$	$\text{C}_\gamma$	$\text{C}_\sigma$	$\text{C}_\beta\text{H}_x$	$\text{C}_\sigma\text{H}_y$	$\eta,^d\%$	$\text{C}_\beta\text{H}_x$	$\text{C}_\sigma\text{H}_y$	$\eta,^d\%$
1	H-enol	184.07	97.16	194.48	25.61	182.10	96.88	194.16	25.41	6.40	2.17	92	6.63	2.22	79
	H-keto	<i>e</i>	55.00	<i>e</i>	<i>e</i>	194.78	53.67	203.77	30.65	4.11	2.21		4.33	2.26	
	-Li	182.06	95.11	190.83	28.63	179.57	94.23	189.40	29.00	5.91			5.84		
	-Li <sub>2</sub> <sup>f</sup>	170.16	102.29	160.74	79.36										
2	H-enol	184.49	96.80	195.84	46.47	182.31	96.52	195.13	44.98	6.31	3.58	99	6.63	3.81	71
	H-keto	<i>e</i>	<i>e</i>	<i>e</i>	<i>e</i>	195.24	52.44	203.31	49.34	4.13	3.65		4.35	3.95	
	-Li	183.78	95.24	191.68	50.31	181.15	93.86	189.62	48.83	5.87			5.86		
	-Li <sub>2</sub> <sup>f,g</sup>	161.09	104.60	169.40	98.71										
3	H-enol	<i>e</i>	109.19	<i>e</i>	39.86	163.70 <sup>g</sup>	107.70	198.74 <sup>g</sup>	41.59	5.68	2.96	8	5.33	<i>h</i>	52
	H-keto	191.94	61.22	203.25	42.59	191.95	60.10	204.52	41.89	4.12	3.40		3.80	2.76	
	-Li	180.37	107.31	194.01	42.77	179.81	106.10	192.72	<i>h</i>	5.07			5.13		

<sup>a</sup> For  $^1\text{H}$  and  $^{13}\text{C}$  NMR measurements concentrations are  $\sim 0.01$  and  $\sim 0.1$  M, respectively. <sup>b</sup> Lithium bis(trimethylsilyl)amine was used as base. <sup>c</sup> Lithium tetramethylsilane was used as base. <sup>d</sup> Percent of the enol form determined by  $^1\text{H}$  NMR. <sup>e</sup> Signals were not detected. <sup>f</sup> Broad. <sup>g</sup> Major isomer. <sup>h</sup> Under DMSO-*d*<sub>6</sub> signal.

**FIGURE 4.** Decoupled  $^{13}\text{C}$  NMR spectra of 1 (A), 1-Li (B), and 1-Li<sub>2</sub> (C) in THF-*d*<sub>8</sub> at 25 °C. Expanded decoupled (D) and coupled (E) spectra of 1-Li<sub>2</sub>.

Information) and 6, respectively. In THF only the  $\text{C}_\beta$  and  $\text{C}_\delta$  carbons of the minor enol form (8%) were detected. All of the other signals are either isochronous with those of the ketone tautomer or too weak to be detected. On the other hand, three sets of resonances were clearly detected for the DMSO-*d*<sub>6</sub> solution of **3** at 25 °C. This is clearly shown in the expanded region (spectrum C) in

Figure 6, which corresponds to the  $\text{C}_\alpha$  and  $\text{C}_\gamma$  carbon signals. The three equilibrating species can be associated with the keto form of **3** and its nonequivalent enol isomers (Scheme 4). The detection of both enol forms of **3** undoubtedly results from the much slower external proton transfer involved with hydrogen bonding to solvent.

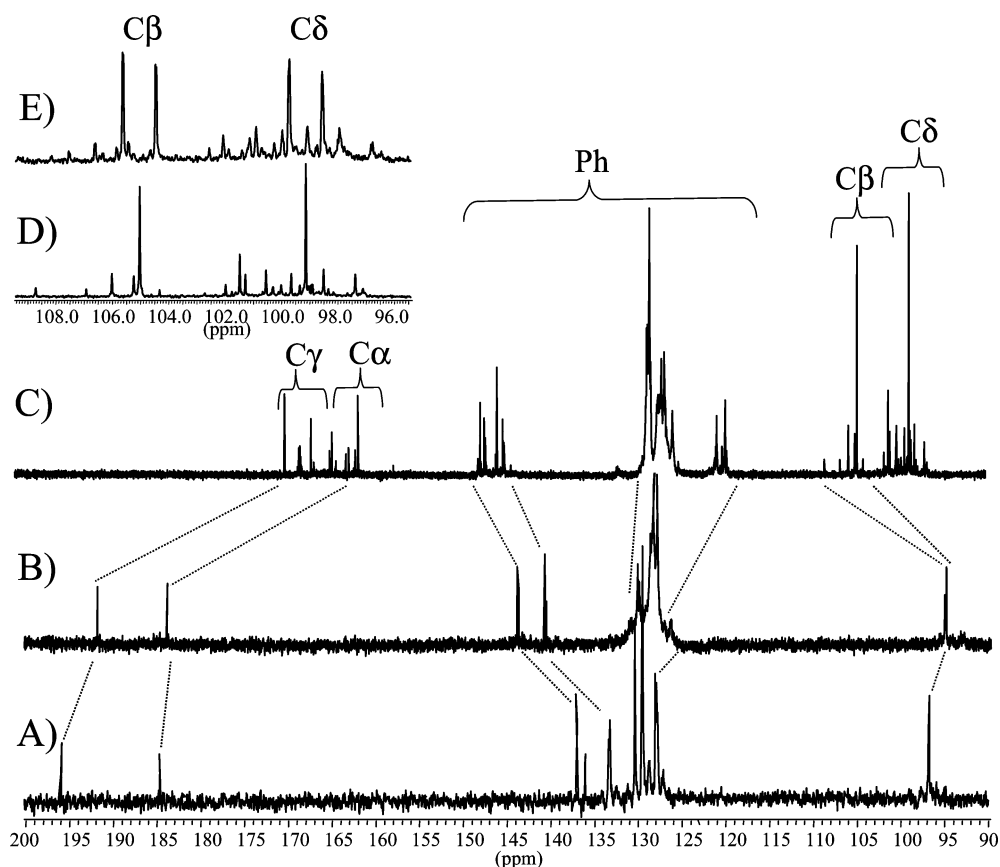


**FIGURE 5.** Decoupled <sup>13</sup>C NMR spectra of **2** (A), **2-Li** (B), and **2-Li<sub>2</sub>** (C) in THF-*d*<sub>8</sub> at 25 °C. Expanded decoupled (D) and coupled (E) **2-Li<sub>2</sub>** spectra.

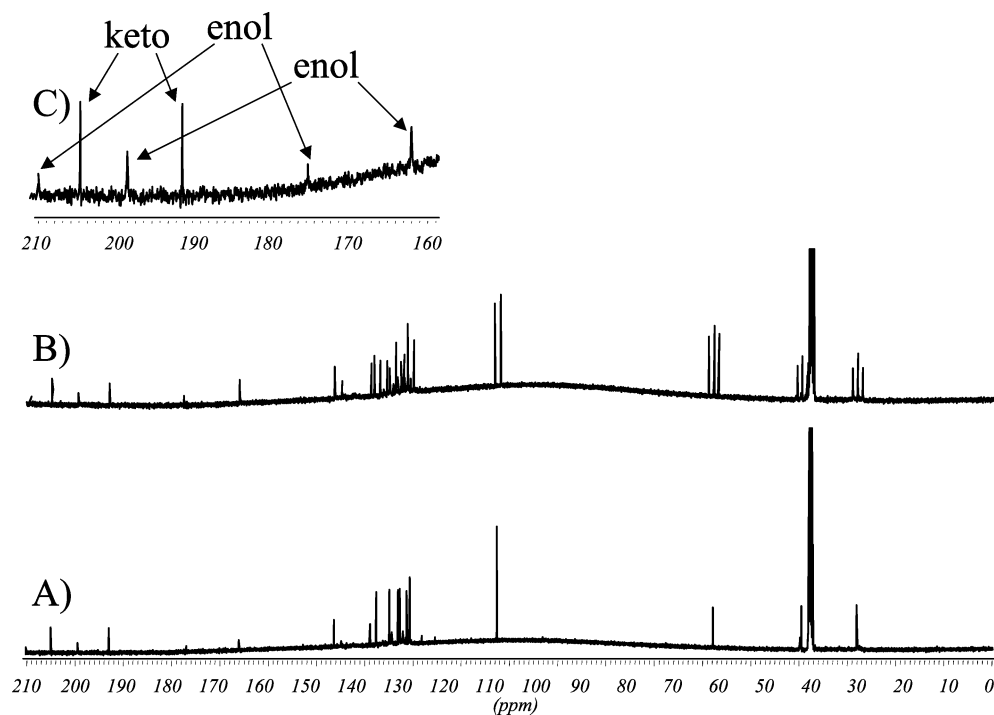
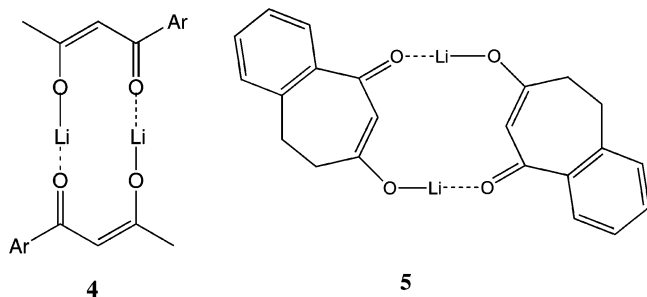


**FIGURE 6.** Decoupled (A) (expanded in part C), and coupled (B) <sup>13</sup>C NMR spectra of **3** in DMSO-*d*<sub>6</sub> at 25 °C.

The <sup>13</sup>C NMR spectra of **1-Li** and **2-Li** in Figures 4 and 5 also exhibit only one set of resonances. A number of possible dimer structures such as that shown as **4** can exist as cis and trans isomers. A single set of resonances

then means that such dimers must interconvert rapidly on the NMR time scale, probably via a rapid equilibrium with monomer. The <sup>13</sup>C NMR spectra of **3-Li** in both THF-*d*<sub>8</sub> and DMSO-*d*<sub>6</sub> also exhibit only one clear set of signals

at room temperature. Two isomeric dimer structures can be proposed for this compound also, one of which is shown in the suggested structure **5**. The fact of a single set of signals suggests a rapid equilibration between them unless the isomers are isochronous. A single set of resonances with minimal variation of the chemical shifts ( $\pm 3$  ppm) was also recorded down to  $-40$  °C in THF- $d_8$  suggesting that the dissociation of **5** is quite facile.



The analysis of the  $^{13}\text{C}$  NMR spectra of the dilithium dienediolates (**1**, **2**)- $\text{Li}_2$  in THF- $d_8$  is more complex. For both systems,  $\text{C}_\alpha$  and  $\text{C}_\gamma$  carbons move substantially to high field whereas  $\text{C}_\beta$  shifts slightly to low field compared to the corresponding conjugate acids. There are apparently two effects operating here. The first is the second deprotonation, which increases electron density on these atoms and should shift their resonances to higher field.<sup>61–64</sup> The second is the  $\text{C}_\delta$  rehybridization and conjugation with the unsaturated moiety to form a diene-like structure. This has a random effect on the carbon olefin frame as seen from the  $^{13}\text{C}$  NMR of the couples ethylene/butadiene, 1-pentene/1,3-pentadiene, and phenylethene/1-phenylbutadiene.<sup>65</sup> The overall chemical shift variations are therefore combinations of these two effects. Finally, there are profound differences in the spectra of **1**- $\text{Li}_2$  and **2**- $\text{Li}_2$ . The spectrum of **1**- $\text{Li}_2$  (Figure 4C) exhibits one single set of broad signals, indicating that at 25 °C the dimer has a single structure or possible isomers undergo fast interconversion (in the NMR scale) but not fast enough for coalescence, which occurs at about 45 °C. Low-temperature experiments, which would have provided information on the number of isomers, could not be performed due to the poor solubility of the enolate. Nevertheless, a reasonable structure for the dimer based on the ubiquitous cube of four oxygens and four lithiums frequently found in X-ray structures of lithium enolates<sup>66–68</sup> can be proposed as shown in **6**. A similar structure was suggested from ab initio MO computations for the dilithium enediolate formed from dideprotonation of a carboxylic acid.<sup>33</sup>

(61) Bradamante, S.; Pagani, G. A. *J. Org. Chem.* **1984**, *49*, 2863.  
(62) Abbotto, A.; Bradamante, S.; Pagani, G. A. *J. Org. Chem.* **1993**, *58*, 449.

(63) Gatti, C.; Ponti, A.; Gamba, A.; Pagani, G. A. *J. Am. Chem. Soc.* **1992**, *114*, 8634.

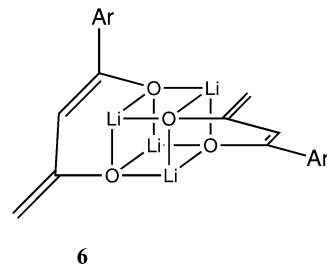
(64) Abbotto, A.; Bradamante, S.; Pagani, G. A. *J. Org. Chem.* **1993**, *58*, 444.

(65) Kalinowski, H.-O.; Berger, S.; Brau, S. In *Carbon-13 NMR Spectroscopy*; John Wiley & Sons: New York, 1988.

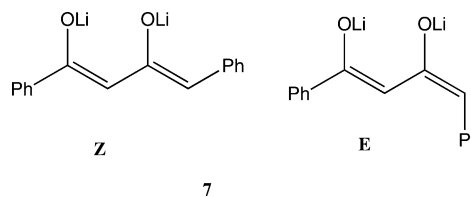
(66) Seebach, D.; Amstutz, R.; Laube, T.; Schweizer, W. B.; Dunitz, J. D. *J. Am. Chem. Soc.* **1985**, *107*, 5403–9.

(67) Seebach, D. *Angew. Chem.* **1988**, *100*, 1685–1715.

(68) Williard, P. G.; Salvino, J. M. *Tetrahedron Lett* **1985**, *26*, 3931–4.



In this structure, unlike that of **4**, there is no role for cis–trans isomerism. However, the monomer of **2**- $\text{Li}_2$  can exist as *E,Z* isomers as shown in **7**. Thus, a cubic dimer



as in **6** could consist of *EE*, *EZ*, and *ZZ* species. These isomers could account for the extra signals in the  $^{13}\text{C}$  NMR spectrum of **2**- $\text{Li}_2$ . Moreover, this compound has a relatively low  $K_d$  and some of the minor signals could arise from the two isomeric *E,Z* monomers. This requires that the dilithio species, unlike the monolithium enolates, dissociate slowly on the NMR time scale. In this connection, we recall that proton-transfer equilibria of **1**- $\text{Li}_2$  and **2**- $\text{Li}_2$  are quite slow, taking hours to reach equilibrium. Similarly, the dimer of the dilithium enediolate from a carboxylic acid is also very tight and dissociates slowly.<sup>33</sup>

## Discussion

The cesium ion pair  $\text{p}K$  values of the indicators in THF are generally close to the  $\text{p}K_a$  values in DMSO.<sup>41</sup> For the cesium salts of enolates, the  $\text{p}K$  values relative to such indicators tend to be about 1  $\text{p}K$  unit less than the DMSO  $\text{p}K_a$  values.<sup>23,25,28,69</sup> In the present cases of the cesium salts of  $\beta$ -diketones, the  $\text{p}K$  of the cesium salt of the enol of **1**, 10.9, is 3.3 units less than that of  $\text{PhCOCH}_2\text{COCH}_3$  in DMSO, 14.2.<sup>70</sup> The latter value is consistent with that of dibenzoylmethane in DMSO, 13.35,<sup>71</sup> which is expected to be a little lower because of the inductive effect of the second benzene ring. The cesium ion pair  $\text{p}K$  of **2** is slightly lower than that of **1** again because of the inductive effect of the second benzene ring now one atom farther removed. The lower ion pair  $\text{p}K$  values compared to ionic  $\text{p}K_a$  values in DMSO show that even the large cesium cation has a significant chelating stabilization effect within the ion pairs. This result is also consistent with the earlier finding by DePalma and Arnett<sup>72</sup> that cesium  $\beta$ -ketoenolates have significant ion pair association constants even in DMSO. No such chelating stabilization should apply to the cesium salt of **3** because of the W-shape of its enolate ion. No comparable compounds

(69) Ciula, J. C.; Streitwieser, A. *J. Org. Chem.* **1992**, *57*, 431–432; correction p 6686.

(70) Personal communication quoted in [www.cem.msu.edu/~reusch/OrgPage/Tables.htm](http://www.cem.msu.edu/~reusch/OrgPage/Tables.htm).

(71) Olmstead, W. N.; Bordwell, F. G. *J. Org. Chem.* **1980**, *45*, 3299–305.

(72) DePalma, V. M.; Arnett, E. M. *J. Am. Chem. Soc.* **1978**, *100*, 3514–3525.

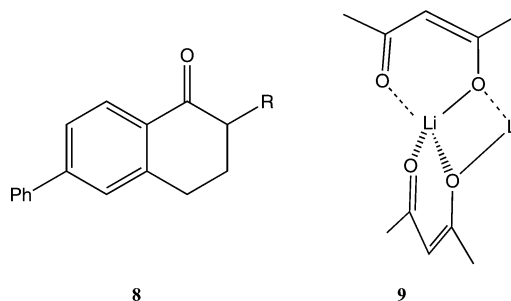
have been studied in DMSO but the ion pair values in THF,  $\sim 12$ – $13$ , are comparable to (and even somewhat higher than) the ionic  $pK_a$  values of 1,3-cyclohexanedione, 10.3, and dimedone, 11.2, in DMSO.<sup>73</sup> These conclusions will probably also apply to the more common potassium salts.

These same considerations also apply to the lithium ion pairs except that chelation effects are now much stronger. Ion pair  $pK$  values of the lithium salts of the delocalized indicators are comparable to the corresponding Cs  $pK$  values because the lithium salts, as solvent-separated ion pairs (SSIP), are effectively only somewhat larger than the cesium contact ion pairs (CIP) and both are relative to the same standard.<sup>43</sup> Lithium ion pair  $pK$  values of enolate ions are 6–9  $pK$  units lower than the corresponding cesium enolates,<sup>23,29,74</sup> because the lithium salts are now CIP electrostatically bound more firmly to the negative enolate oxygens. One would therefore expect that the corresponding  $\Delta pK$  values for  $\beta$ -ketoenolates would be still greater, but in fact the values shown in Table 4, about 8, are of the same magnitude. The unequal O–M bond distances in the  $\beta$ -ketoenolate chelates undoubtedly play a role together with the fact that the two oxygens in the  $\beta$ -ketoenolate ions effectively share a single negative charge.

The second  $pK$  values of the  $\beta$ -diketones are, of course, much higher than the first. For the lithium and dilithium salts of **1** the difference (Table 3) is about 19  $pK$  units. The difference drops to about 15 for **2**; the  $pK_2$  difference of 4.2 between **1**-Li<sub>2</sub> and **2**-Li<sub>2</sub> shows the effect of conjugation; the second anion in **2**-Li<sub>2</sub> is now benzylic. Indeed, the value of 17.7 for **2**-Li<sub>2</sub> is remarkably low for a dianion; it is not much greater than the  $pK$  for the monomer lithium salt of *p*-phenylisobutyrophenone, 15.9.<sup>31</sup> The  $pK_2$  for the corresponding dicesium salt, **2**-Cs<sub>2</sub>, 24.5, is higher by an amount typical of the difference between lithium and cesium salts of monoketones. For example, the  $pK$  for the monomer of the cesium salt of *p*-phenylisobutyrophenone is 25.1.<sup>25</sup>

The aggregation of lithium enolates in THF is affected generally by steric effects and by basicity. For example, 6-phenyl- $\alpha$ -tetralone, **8** (R = H), and its 2-benzyl derivative, **8** (R = benzyl), have comparable ion pair lithium basicities but the less hindered enolate aggregates to a tetramer whereas the more hindered benzyl derivative forms a dimer.<sup>30</sup> The lithium salt of *p*-phenylisobutyrophenone aggregates to a tetramer<sup>31</sup> but less basic enolates that are also derived from ketones with a tertiary  $\alpha$ -hydrogen often form dimers instead. These dimers have  $K_d$  values of the order of  $10^3 \text{ M}^{-1}$ ,<sup>27–29</sup> similar to those of **1**-Li and **2**-Li. In the case of the lithium enolates of monoketones, part of the driving force for dimerization is the entropy gained by loss of solvation of the lithium. For the chelated lithium enolates of  $\beta$ -diketones, the lithiums are less solvated to begin with and this driving force should be lower. The lithium in a nonchelated enolate, such as **3**-Li, is then more highly solvated and has more solvation entropy to gain on dimerization. Accordingly,  $K_d$  for **3**-Li is much higher,  $26\,000 \text{ M}^{-1}$ . The structures of the dimers are not known

but, as discussed above, reasonable structures are exemplified in **4** and **5**. An alternative structure **9** is a



twisted version of **4** and is a portion of a polymeric crystal structure of unsolvated lithium acac. This structure, however, seems less reasonable for the dimer in solution because of the reduced possibilities for solvation of lithium cation. In both structures **4** and **9** the lithiums are probably less solvated than in the chelated monomer and loss of solvation provides some driving force for dimerization. In **5**, however, the reduced solvation of the lithiums compared to the nonchelated monomer of **3**-Li probably provides much of the driving force for the higher value of  $K_d$ . Coordination solvation of the lithiums in these structures has not been included in the proposed structures but all of the lithiums are probably three- or four-coordinate with inclusion of ether solvents.<sup>73</sup>

For the monomeric dimetal dienediolates a reasonable structure would be **10**, which features the cyclic Li<sub>2</sub>O<sub>2</sub> bonding common in lithium enolate dimers.<sup>75</sup> Such a monomer structure could readily dimerize to the cubic structure **6**. In this dimerization the reduced basicity of **2**-Li<sub>2</sub> and the greater steric hindrance provided by the terminal phenyl group would both lead to a lower  $K_d$  compared to that of **1**-Li<sub>2</sub>.



Finally, the structural speculations presented here have been confirmed by ab initio computations to be published separately.<sup>76</sup>

## Conclusions

$\beta$ -Diketones that can lead to chelated monoalkali salts have relatively high ion pair acidities and dimerization constants comparable to those of simple enolates, of the order of  $10^3 \text{ M}^{-1}$ . Thus, THF solutions of such compounds in typical synthetic reactions or physical measurements (such as NMR) of 0.01 M or more consist mostly of dimers but the possible role of such dimers is rarely considered.  $\beta$ -Diketones whose anions are W-shaped and cannot give intramolecular chelates are less acidic but only by about 2  $pK$  units. Their enolates, however, have larger aggregation constants by another order of magnitude. Derived dilithium dienediolates have relatively low ion pair  $pK$

(73) Arnett, E. M.; Harrelson, J. A., Jr. *J. Am. Chem. Soc.* **1987**, *109*, 809–812.

(74) Wang, D. Z.; Streitwieser, A. *J. Org. Chem.* **2004**, *68*, 8936–8942.

(75) Pratt, L. M.; Streitwieser, A. *J. Org. Chem.* **2003**, *68*, 2830–2838.

(76) Manuscript in preparation.

values and comparable dimerization constants. Corresponding cesium salts generally are somewhat less aggregated.

## Experimental Section

**General.** Melting points (Pyrex capillary) were determined on a Buchi melting point apparatus and are uncorrected. UV-vis spectra were recorded on a spectrophotometer equipped with fiber optics cables connected to a thermostated cell holder built into the floor of the glovebox.

**Materials.** Starting materials for synthesis were obtained from commercial suppliers and purified by crystallization or distillation prior to use. Purity of synthesized compounds was monitored by combination of  $^1\text{H}$  NMR, GLC, mp, and elemental analysis.

**1-(4-Biphenyl)butane-1,3-dione, 1:** Prepared following Sprague,<sup>39</sup> 55% yield, white solid, mp 160 °C (after sublimation) (lit.<sup>39</sup> mp 156–7 °C). Anal. Calcd for  $\text{C}_{16}\text{H}_{14}\text{O}_2$ : C, 80.65; H, 5.92. Found: C, 80.42; H, 5.90.

**1,4-Diphenylbutane-1,3-dione, 2:** Prepared following Padwa,<sup>40</sup> 61% yield, white solid, mp 56 °C (after sublimation) (lit.<sup>40</sup> mp 52–3 °C). Anal. Calcd for  $\text{C}_{16}\text{H}_{14}\text{O}_2$ : C, 80.65; H, 5.92. Found: C, 80.51; H, 5.98.

**6,7,8,9-Tetrahydro-5H-benzocyclohepten-5,7-dione, 3.** Potassium *tert*-butoxide (0.34 g, 3.00 mmol) was added to a solution of ethyl  $\beta$ -(2-acetylphenyl)propionate (0.30 g, 1.36 mmol) in dry *tert*-butyl alcohol (40 mL). After refluxing for 45 min, the reaction mixture was poured onto water (70 mL) and  $\text{H}_2\text{SO}_4$  (20%) was added until the pH was brought to about 1. The aqueous solution was extracted with ether and the organic layer was dried ( $\text{MgSO}_4$ ) and evaporated to afford a brown solid (380 mg). The solid was chromatographed on silica gel ( $\text{Et}_2\text{O}$ :  $\text{AcOEt}$  9:1) to afford the target compound as a white solid (0.17 g), which was obtained analytically pure after sublimation (0.15 g, 0.86 mmol, 63%); mp 61 °C.  $^1\text{H}$  NMR ( $\text{CDCl}_3$ )  $\delta$  7.97 (d,  $J$  = 7.8 Hz, 1H), 7.51 (t,  $J$  = 7.5 Hz, 1H), 7.38 (t,  $J$  = 7.4 Hz, 1H), 7.27 (d, 1H), 4.13 (s, 2H), 3.37 (t,  $J$  = 6.2 Hz, 2H), 2.76 (t, 2H). Anal. Calcd for  $\text{C}_{11}\text{H}_{10}\text{O}_2$ : C, 75.83; H, 5.80. Found: C, 75.67; H, 5.58.

**Deprotonating Agents.** The solutions of cesium diphenylmethane and cumyl cesium used to prepare the cesium enolates were obtained according to known procedures.<sup>35</sup> Trimethylsilylmethyl lithium was prepared following the method described by Saljoughian.<sup>77</sup> After sublimation, it was transferred into the glovebox and used as a solid to prepare the lithium enolates. Lithium diisopropylamide (Aldrich) was sublimed three times before use.

**Extinction Coefficient Measurements.** A solution of known concentration of **1–3** in THF was prepared in a UV

cuvette, and an excess of base was added to have the neutral compound completely either mono- or dideprotonated. The solution was successively diluted with known amounts of THF, and the spectrum was obtained after each dilution with the extinction coefficient at each concentration calculated in a straightforward manner.

**Acidity Measurements. Single indicator method:** A known amount of hydrocarbon indicator was transferred into a thermostated 0.1 or 1 cm quartz cell containing a known amount of THF. The base was added and the UV-vis spectrum was immediately recorded. A known amount of substrate (**1–3**) was added and the mixture was left to reach equilibrium. Dilution with known amounts of THF provided spectra at different anion concentrations. **Double indicator method:** A known amount of both an appropriate indicator and a substrate (**1–3**) were transferred into a thermostated 0.1 or 1 cm quartz cell containing a known amount of THF. At this point two procedures were followed depending on whether the equilibrium between the indicator and the substrate was reached rapidly or slowly. In the first case a small amount of base was added and the spectrum of the solution was immediately recorded. In the second, the base was added until the absorbance of the solution reached 1.5–2.0 absorbance units, then the mixture was left to reach equilibrium. Spectra at different anion concentrations were obtained by successive addition of base in the first case or by dilution with known amounts of THF in the second case..

**NMR Measurements.** THF- $d_6$  and DMSO- $d_6$  were dried by distillation from Na/K alloy and  $\text{CaH}_2$ , respectively.  $^1\text{H}$  and  $^{13}\text{C}$  NMR spectra were recorded at 25 °C with a spectrometer operating at 125.70 MHz in the FT mode. The spectral parameters and calibration were set according to known procedures.<sup>78</sup> When possible, the samples were investigated as 0.01 and 0.1 M solutions for  $^1\text{H}$  and  $^{13}\text{C}$  spectra, respectively.

**Acknowledgment.** This research was supported in part by grants from the National Science Foundation.

**Supporting Information Available:** Figures S1–S25 showing UV-vis spectra for **1**, **2**, and **3**, plots of absorbance for **1**, **2**, and **3**, plots of  $K_{\text{obs}}$  vs {enolate}/ $K_{\text{obs}}$  for **1**-Li, **2**-Li, **3**-Li, **1**-Cs, and **2**-Cs, plots of  $K_{\text{obs}}$  vs {**1**-Li<sub>2</sub>}/ $K_{\text{obs}}$ , {**2**-Li<sub>2</sub>}/ $K_{\text{obs}}$ , and {**2**-Cs<sub>2</sub>}/ $K_{\text{obs}}$ ,  $^1\text{H}$  NMR spectra for **1**, **2**, and **3**, and  $^{13}\text{C}$  NMR spectra for **3**; Tables S1 and S2 with properties of regression lines and equilibrium constants of the enol/keto equilibrium for **1–3**. This material is available free of charge via the Internet at <http://pubs.acs.org>.

JO0491915

(78) Abbotto, A.; Alanzo, V.; Bradamante, S.; Pagani, G. A. *J. Chem. Soc., Perkin Trans. 2* **1991**, 481.

(77) Saljoughian, M. *Monatsh. Chem.* **1984**, *115*, 519.